ECS Transactions, 114 (5) 325-336 (2024)
10.1149/11405.0325ecst ©The Electrochemical Society

Effect of Non-ionic Surfactant on Fe-N-C Catalyst Layers under HT-PEMFC Conditions

Tanja Zierdt[a,b], Jonas Knake[a,c], Julia Müller-Hülstede[a], Dana Schonvogel[a], Peter Wagner[a], Michael Wark[c] and K. Andreas Friedrich[b,d]

[a] Institute of Engineering Thermodynamics, German Aerospace Center (DLR), Oldenburg 26129, Germany
[b] Institute for Building Energetics, Thermotechnology and Energy Storage (IGTE), University of Stuttgart, Stuttgart 70569, Germany
[c] Institute of Chemistry, Carl von Ossietzky University, Oldenburg 26129, Germany
[d] Institute of Engineering Thermodynamics, German Aerospace Center (DLR), Stuttgart 70569, Germany

The effect of different non-ionic surfactant contents on Fe-N-C gas diffusion electrode (GDE) coating and performance is investigated. GDEs are tested under high temperature polymer electrolyte membrane fuel cell (HT-PEMFC) conditions at 160 °C and concentrated phosphoric acid electrolyte. Fe-N-C-based GDEs are fabricated through ultrasonic spray coating with Tergitol contents of 0, 1, 20 and 50 wt% in the catalyst layer (CL). Thereby, the PTFE to catalyst ratio is kept constant at 1.0 in the CL. The H_2O contact angle decreases with increasing Tergitol™ content in the CL, revealing an increased wettability. H_3PO_4 contact angles of Tergitol containing GDEs show a same wettability at room temperature as at 160 °C. GDE half-cell setup investigations show, that Tergitol leads to flooding of the electrode by the electrolyte and coverage of the active sites by the surfactant and thus a performance decay.

Introduction

This is important to reduce the cost of the HT-PEMFC as this technology presents is promising for heavy-duty, aircraft, and maritime applications and operates at around 160 °C.(1) The electrodes of the HT-PEMFC are usually based on Pt nanoparticles on carbon blacks, but phosphate ions from the phosphoric acid doped polybenzimidazole (PBI) membrane can partly poison the Pt surface.(2) This unwanted effect requires high Pt loadings up to 1 mg_{Pt} cm^{-2} per electrode and comes along with higher material costs in comparison to lower Pt loadings of approx. 0.4 mg_{Pt} cm^{-2} for low temperature (LT)-PEMFCs.(2) Metal-nitrogen-carbon (M-N-C) catalysts are promising candidates for replacing expensive and rare Pt for catalyzing the oxygen reduction reaction (ORR) at the cathode.(1) At present, the most promising type of Pt-free M-N-C catalyst is Fe-N-C, which has the potential to noticeably diminish the financial outlay associated with the manufacture of PEMFCs.(3) They have shown comparable ORR activity to Pt/C in acidic electrolyte in rotating disk electrode measurements.(4, 5) Also, Fe-N-Cs are not expected to be affected by phosphate poisoning. It is shown that phosphate ions adsorption near active sites promotes ORR by suppling protons.(1, 6-8)

Fe-N-C characteristics in terms of active site density, porosity, wettability and surface functionalization are different from Pt-based catalysts, and thus, the requirements of electrode composition cannot be directly transferred. The electrode constitution, in which significant parts of the active sides should be connected to thin film of phosphoric acid leaving the pores open enough for gas transport is crucial for the HT-PEMFC performance.(9) An optimal pore network is required for good transport of oxygen and protons.(10) Thus, the Fe-N-C catalyst demands investigations of catalyst layer (CL) properties with regard to its fabrication and the CL wettability. In a previous study, we demonstrated the feasibility of Fe-N-C-based GDEs for ORR under HT-PEM conditions (conc. H_3PO_4, 160 °C) and also pointed out the demand for improving the CL morphology.(3) We showed that Fe-N-C catalyst is feasible to maintain performance within a wide range of PTFE contents from 20 to 50 wt% in the CL.(2)
Non-ionic surfactants can enhance the wetting of the CL, as Mack et al. found by a reduced break-in time of Triton complemented Pt/C electrodes in HT-PEMFC operation.(11) Furthermore, Lee et al. reported improved dispersion of PTFE binder within the catalyst ink due to employed non-ionic surfactant and increased the HT-PEMFC performance of the Pt-based electrode.(12) However, Triton is less relevant for industrial use as it is listed as substance of very high concern (SVCH) by REACH regulation, according to annex XVII of article 59(10) of Regulation (EC) 1907/2006 (REACH).
This study reports Fe-N-C-based (PMF-D14401, Pajarito Powder) GDEs, fabricated by ultrasonic spray coating with Tergitol contents of 0, 1, 20 and 50 wt% in the CL and a constant PTFE to catalyst ratio of 1.0. Interconnection of PTFE and catalyst material should be ensured by the surfactant. The results include the determination of the iron content of GDEs by inductively coupled plasma mass spectrometry (ICP-MS) and scanning electron microscopy (SEM) to compare CL morphologies along all GDEs. Furthermore, the electrode performances are accessed by hot pressing a H_3PO_4 doped polybenzimidazole membrane onto the CL and subsequent electrochemically characterization in a half-cell setup under HT-PEMFC condition at 160 °C in conc. H_3PO_4 electrolyte.

Experimental Part

GDE fabrication

A commercial Fe-N-C catalyst (PMF-D14401, Pajarito Powder) was used for GDE fabrication. The catalyst powder was mixed with ultrapure water and 2-propanol and Tergitol (composition see Table I), sonicated for 15 min using an ultrasonic (US) horn (amplitude 15 %, on: 30 s, off: 10 s) while keeping the suspension cooled in an ice-bath. This suspension was then mixed on a roller mixer RS-TR 10 (Phoenix Instrument) overnight. Afterwards, it was sonicated in an ice-cooled US-bath for 10 min, followed by addition of PTFE-dispersion according to Table I.

The mixture was horn-sonicated (same conditions) and immediately transferred to the US spray coating device ExactaCoat (Sono-Tek) equipped with a 48 kHz nozzle. A gas diffusion layer (GDL) with microporous layer (MPL) (H23C2, Freudenberg) served as substrate and was placed on a heating plate at a temperature of 40 °C. The catalyst suspension was sprayed on an area of 5x5 cm² layer by layer in serpentine shape (rotated by 90° after each layer) with a flow rate of 0.2 mL min^{-1} including a drying step with

nitrogen gas flow of 0.3 kPa after each layer. The suspension was sonicated within its reservoir during the drying step. The targeted Fe-N-C loading was 3 $mg_{Catalyst}$ cm^{-2} for each GDE. For higher amounts of Tergitol, the masses of water and 2-propanol were varied to keep the solid-liquid ratio constant (Table I). The GDEs were stored under nitrogen atmosphere until use.

TABLE I. Composition of the catalyst suspension and GDE notation.

GDE notation	0 wt%	1 wt%	20 wt%	50 wt%
Catalyst / wt%	50			
PTFE / wt%	50			
Surfactant/catalyst ratio	0.00	0.01	0.25	1.00
PTFE/catalyst ratio	Ca 1.00			
Solid/liquid ratio	Constant at 2.90			
Water/2-propanol ratio	Constant at 0.30			
Number of coating layers	298			

Sedimentation analysis

The sedimentation of the catalyst suspensions with Triton and Tergitol was determined by the dry mass of a defined volume. For this purpose, catalyst suspensions with 0, 1, 20 and 50 wt% Tergitol were prepared as described before. These catalyst suspensions were stored in a closed screw-top jar for 60 min. This time period was chosen as the ultrasonic spray coating process needs approx. 149 min for applying the catalyst suspension onto the GDL. Strong sedimentation after 60 min would lead to such inhomogeneous CL application, that GDE reproducibility in terms of targeted catalyst loading is highly limited. After 60 min a volume of 100 µL of the suspension was removed at a distance of 1.5 cm from the meniscus. The removed volume of suspension was pipetted into an empty screw-top jar and dried at 40 °C for 16 h. The amount of additive was then subtracted from the weighed mass. The proportion of PTFE could be neglected at this point, as it remains constant.

GDE half-cell measurement

With a two-pillar press TRG-2 (P/O/Weber) a phosphoric-acid doped PBI membrane Celtec®-P (BASF) was hot-pressed with 1 kN for 30 s at 140 °C with the CL side of the GDE. The membrane was stored several days in 50 vol% H_3PO_4 before use. Shim shields of around 80 % of the initial thickness of the GDE and membrane protected the GDE/membrane from crushing. Afterwards, the GDE/membrane was fixed in the half-cell being ready for measurements.

The half-cell measurements were performed using the commercial FlexCell® PTFE (Gaskatel). The cell construction was modified with a PTFE shield to give a limited geometric active area of 0.785 cm^2 saving material and enabling higher current densities. Furthermore, a copper plate leaving the geometric active area free was placed on the GDL-side of the GDE to enhance electrical conductivity. The GDE (working electrode, WE), the copper plate and the PTFE shield were sandwiched between two silicon sealings and placed between the electrolyte and gas. After cell assembling, the gap between the two cell compartments was sealed with PTFE tape to prevent unwanted gas penetration to the GDE. 40 mL of conc. phosphoric acid (85 % H_3PO_4 for analyse, Merck) served as electrolyte. As counter electrode (CE) a Pt coil and as reference electrode a reversible

hydrogen electrode (RHE) (HydroFlex™ 81010, Gaskatel), which was frequently calibrated against a H_2/Pt electrode, were used. The cell was heated to 160 °C with heating elements inside the cell body regulated by the temperature control box (Gaskatel). Before measurements, all compartments were rinsed with ultrapure water and 2-propanol (≥99.5% for synthesis, Carl Roth) and dried.

Electrochemical measurements were performed using the potentiostat Modulab2100A (Ametek) equipped with a 12V/20A external booster (Ametek). From each GDE at least two pieces were cut followed by two half-cell tests for each type of GDE containing different amounts of surfactant. Cyclic voltammograms (CVs) were recorded as follows. Nitrogen with a flow rate of 130 mL min^{-1} was led through the gas compartment starting 15 min before and maintained during CV recording. Simultaneously, nitrogen was led into the electrolyte compartment to remove and keep the electrolyte free from oxygen. The CV-procedure consists of three cycles for each scan rate of 20, 50 and 100 mV s^{-1} between 0.05 and 1.05 V_{RHE}. An electrochemical impedance spectrum (EIS) from 0.1 Hz to 300 kHz at 0.5 V_{RHE} with an amplitude of 0.05 V_{RHE} was recorded, where the uncompensated resistance (R_u) was extracted at the intercept with the x-axis or the minimum. The CVs were recorded again with same parameters but with in-situ compensation of the *iR*-drop of 95 %. These CVs were recorded before the polarization curves and assigned as "begin of test" (BoT). With same parameters CVs were recorded after polarization curve measurements and assigned as "end of test" (EoT). The protocol for polarization curves was adapted from Ehelebe et al..[33] First, oxygen with a flow rate of 150 mL min^{-1} was led through the gas compartment of the cell for at least 20 min or until stable (fluctuation <0.1 mV) open circuit potential for more than five minutes. Galvanostatic steps are applied for 30 s for currents (i) from -0.02 mA to -360 mA and for 5 s from -0.470 A to -1.57 A. The shorter holding time was chosen to minimize the increase in temperature due to the higher reaction rates. Each current step was directly followed by EIS at the same current density. The frequency range was set in a range from 0.1 Hz to 300 kHz with amplitudes from 1 up to 800 mA and increases with increasing current density. The last 3 s of the recorded potential at each current step were averaged and afterwards *iR*-drop corrected ($E_{iR\_corrected} = E_{uncompensated} - i * R$). R was extracted from EIS from either the intersection with the x-axis or the minimum of the spectra.

Contact angle determination

Contact angle measurements were carried out with the device OCA25 (Dataphysics). Drops (9 µL) of ultrapure water or conc. phosphoric acid (85 vol% H_3PO_4 Emsure® Merck) were deposited via a blunt cannula onto the CL of a horizontal aligned GDE under ambient conditions. For water a cannula of 0.25 mm and for conc. phosphoric acid of 0.50 mm inner diameter was used. For the measurement of the contact angle at 160°C, the temperature chamber PC 160U (Dataphysics) was used. The contact surface of the GDE was heated to 160°C and the GDE was placed inside the temperature chamber. The ambient temperature was approx. 90°C. The contact angles were measured 10 s after the drop was applied to the GDE. Analysis of contact angles was done using Young-Laplace fitting within dpiMAX Software (Dataphysics). The H_2O and H_3PO_4 contact angles of six independent measurement points were averaged for each electrode.

Determination of iron content

To examine the iron content in the GDEs inductively coupled plasma mass spectrometry (ICP-MS) was conducted with the iCap Qc (Thermo Fisher Scientific). Alongside to 15 mg the PMF-D14401, Pajarito Powder Fe-N-C catalyst, for each Fe-N-C GDE a 1 cm^2 piece was punched out, digested in 2 mL concentrated HNO_3 (Rotipuran®Supra 69 wt%, Carl Roth) and boiled for 1 h. The solution was stored overnight. Then, the sample was filtrated and the filtrate volume was adjusted to 50 mL by addition of ultrapure water. 10 µL of a scandium internal standard (1,000 mg L^{-1}, ROTI®Star 1, Carl Roth) was added to 10 mL of the sample solution. The calibration solutions consist of a Fe ICP standard (Carl Roth) with concentrations of 0, 0.2, 0.5, 1, 2, 3 and 4 mg L^{-1}. A correlation coefficient of at least 0.999 was ensured during external calibration. The Fe-N-C loading was calculated by correlating the iron content of the catalyst powder to the determined iron content of the CL.

Scanning electron microscopy (SEM)

The surface morphology and elemental composition of the GDE surface was analyzed with SEM. GDEs pieces of about 0.5 x 0.5 cm were placed onto carbon tape on an aluminum sample holder and placed in the SEM Hitachi S-3200N (Hitachi Ltd.) for acquiring of the SEM micrographs. The microscope was operated at an acceleration voltage of 20 kV in high vacuum.

Results and Discussion

Four different non-ionic surfactant contents of 0, 1, 20 and 50 wt% are investigated as additive for Fe-N-C GDE fabrication. The GDE with 0 wt% Tergitol serves as reference GDE without any surfactant. The commercial Fe-N-C catalyst type PMF-D14401 (Pajarito Powder) and a constant PTFE/catalyst ratio of 1.0 is used. First, the effect on ink stability of the two non-ionic surfactants Triton X-100™ and Tergitol 15-S-19™ is investigated in comparison by sedimentation analysis. No strong difference in sedimentation behavior is observed between the catalyst suspensions prepared with Triton and Tergitol. Therefore, further steps are carried out with more environmentally friendly Tergitol. It is noticed, that sedimentation occurred for the reference catalyst suspension with 0 wt% Tergitol. After 60 min sedimentation increases with increasing Tergitol amount by a small portion of 24 % (1 wt%), 29 % (20 wt%) and up to 39 % (50 wt% Tergitol GDE).

Morphology and composition of the CL

It firstly needs to be ensured that the CL application and GDE fabrication is reliable and homogenous when adding the non-ionic surfactant as additive. Therefore, the composition and morphological character are investigated.
The catalyst loading of the GDEs in TABLE II is determined by weight and ICP-MS. For the latter, the loading is estimated from detected iron content in the GDE and correlated to the catalyst iron content of 0.5 wt%. The catalyst loadings are in a similar range for all GDEs and close to the target loading of 3 mg cm^{-2}. This ensures reliable CL application for all Tergitol contents as strong sedimentation of the catalyst suspension in the ink reservoir or the tubes would lead to lower Fe-N-C loading, which not occurred in significant amount here. However, lower Fe-N-C loading is noticeable for the GDEs that

contain Tergitol. This is in line with the observed increase in sedimentation. But the effect seems to be negligible.

TABLE II. Fe-N-C content of the GDEs.

Tergitol content in CL / wt%	Fe-N-C loading, ICP-MS / mg cm^{-2}
0	3.0
1	2.7
20	2.8
50	2.8

SEM images in Figure 1 depicts the CL surface for all Tergitol contents. The CL surface shows the typical porous, rough surface of GDEs similar to other studies on ultrasonic spray coated electrodes.(2, 13) This shows, that CL fabrication is possible with different Tergitol contents even though sedimentation occurred.

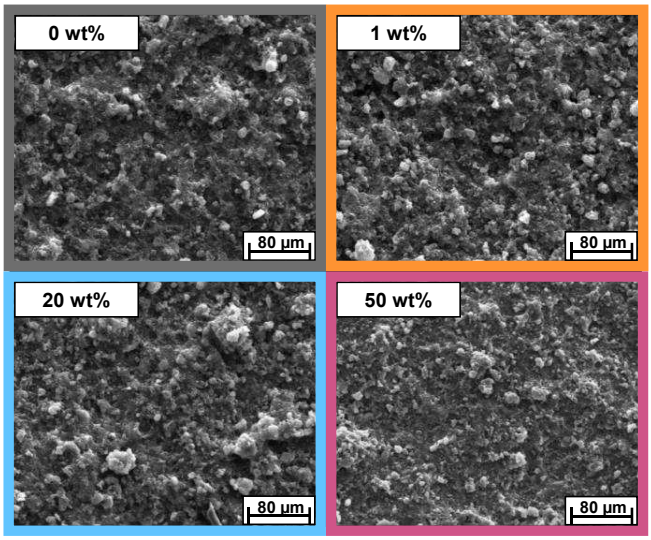

Figure 1. SEM images of CL surface for different Tergitol contents.

Wettability of the GDEs

The wettability of the CL with H_2O and conc. H_3PO_4 plays an important role during HT-PEMFC operation.(2) The contact angle of the CL with H_2O in Figure 2 reveals similar contact angle of the 0 and 1 % Tergitol GDEs. With increasing Tergitol content of 20 and 50 % the contact angle decreases by 60 % and 85 %. H_2O immediately soaks into the CL of the 50 wt% Tergitol GDE. The same trend is visible for the H_3PO_4 contact angles at room temperature. For the wetting behaviors of the CL at room temperature it can be concluded that, with increasing Tergitol content the wettability with H_2O and H_3PO_4 increases.

Contact angles with H_3PO_4 are also determined at HT-PEMFC relevant temperature of 160 °C. With this special approach the wetting behavior of the CL at HT-PEMFC conditions are imitated. The contact angle of H_3PO_4 of the 0 wt% Tergitol GDE in Figure 2 unveiled a drastic decrease of 39 % from room temperature to 160 °C. The CL wettability with H_3PO_4 of the 0 wt% Tergitol GDE increases with increasing temperature. In contrast, the contact angle for the 1 wt% Tergitol GDE decreased by 4 % only. A decrease of 15 %

is noticed for the 20 wt% Tergitol GDE, while for the 50 wt% Tergitol GDE no significant differences between the H_3PO_4 contact angle at room temperature and 160 °C is observed. For the GDEs with Tergitol contents of 1, 20 and 50 wt% the wettability does not distinctively change from room temperature (RT) to 160°C, whereas the CL wettability of the 0 wt% Tergitol GDE increases with enhanced temperature. Hence, the Tergitol containing CL already provide a sufficiently wetted surface at RT. We furthermore revealed that with increasing Tergitol content the wettability increased for the Fe-N-C based GDEs.

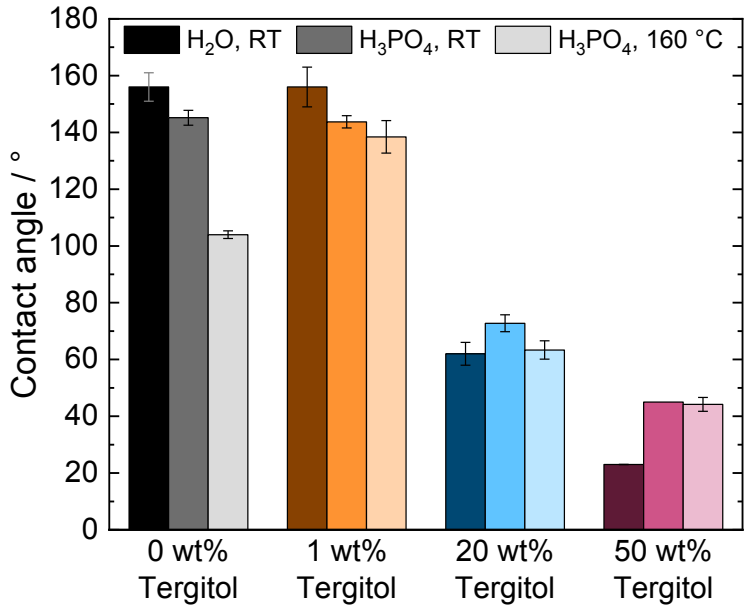

Figure 2. Wetting behavior of the CL of different Tergitol content with H_2O (room temperature) and with conc. H_3PO_4 at room temperature (RT) and at 160 °C.

Halter et al. reported that the contact angles of conc. H_3PO_4 at 160 °C on PTFE is similar to H_2O at room temperature. The contact angle of H_3PO_4 increases with elevated temperature due to higher acid concentration.(14) Compared to our findings, similar contact angle of H_2O at room temperature and H_3PO_4 at 160 °C is only observable for the CLs that contain Tergitol in Figure 2. The wettability of the CL without Tergitol drastically increases at higher temperatures. This depicts that the 0 wt% Tergitol GDE might not be sufficiently or fully wetted at RT. Tergitol ensures wetting properties similar to 160 °C already at room temperature. This is in line with the findings of Mack et al., where Triton was found to shorten the break-in time due to enhanced wetting of the Pt/C electrode CL in the HT-PEMFC.(11)

Although the contact angle can give good indication of the CL wettability, the in-situ wetting and contact angles within the pore network cannot be addressed with this method. Therefore, the performance under HT-PEMFC conditions is examined within the GDE half-cell setup as next step.

GDE half-cell characterization under HT PEMFC conditions

Finally, the performance is accessed by hot pressing a PBI-membrane onto the GDEs and subsequent electrochemically characterization in a GDE half-cell setup, under HT-PEM conditions at 160 °C in conc. H_3PO_4 electrolyte.
Figure 3 represents the CVs, which are recorded before and after the polarization curves. For 0 wt% Tergitol GDE in Figure 3-A no significant differences between CV curve progression at BoT and EoT are observable. The peaks around 0.2-0.4 V_{RHE} (anodic scan) for the CV might be attributed to iron redox couple. Investigations of Wang et al. reveal a shift of iron redox couple peak of Fe-N-C catalyst to lower potentials in H_2SO_4 compared to $HClO_4$ electrolyte, because of the lower adsorption strength of the corresponding anion with iron.(8) As the phosphate anions adsorption strength is smaller than sulphate anions,(8) the peak might be shifted to lower potentials around 0.2-0.4 V. However, literature about the behavior of Fe-N-C cathodes in HT-PEMFC environment is lacking, which leaves understanding of these peaks uncertain. Redox peaks between 0.5 and 0.6 V_{RHE} can be attributed to hydroquinone/quinone species on the one hand and Fe^{2+}/Fe^{3+} redox transitions on the other hand, which are superimposed with the capacitive currents.(3)

For 1, 20 and 50 wt% Tergitol GDE no peaks are detected at BoT in Figure 3-B, C and -D. Tergitol alters the GDE wetting in the half-cell. A significant increase in electrochemical double layer current densities are observed at EoT compared to BoT for the total CV. CVs of 1, 20 and 50 wt% Tergitol at EoT are comparable to the 0 wt% Tergitol GDE. The CVs at EoT and BoT are recorded at the same scan rate, which allows for the conclusion that the higher electrochemical double layer current densities are a result of a larger carbon structure area of the GDEs being wetted with electrolyte. For this phenomenon, two effects are accountable. First, it is possible that the CL was fully flooded at EoT, so that also the carbon of the MPL or GDL is involved. This trend is in line with contact angles in Figure 2, where a higher Tergitol content leads to decreased contact angles which implies an increased electrode wetting. Next, the production of water during ORR leads to dilution of the electrolyte and redistribution of the phosphoric acid water mixture and altered coverage of the CL with electrolyte and flooding of the CL. Second, at BoT the Tergitol partly covered the carbon matrix of the CL, so that a smaller surface is electrochemically available. The differences in BoT and EoT CV curve shape might be traced back to electrochemically and/or chemically leaching of Tergitol from the CL during polarization curve recording. To evaluate this effect a 20 wt% Tergitol GDE was treated at 320 °C for 20 min to (partially) remove the surfactant, as 300 °C is the boiling point of Tergitol. The BoT and EoT CVs stayed the same in the half-cell measurement. Or course, other effects like sintering of PTFE particles and catalyst degradation during heat treatment might influence the CV. However, Tergitol altered the CL so that flooding cannot be inhibited, as visible in increased electrochemical double layer current densities for all Tergitol GDEs at EoT. The uncompensated resistance will give insight into the electric resistance inhibition that occurred in the electrode depending on the Tergitol content.

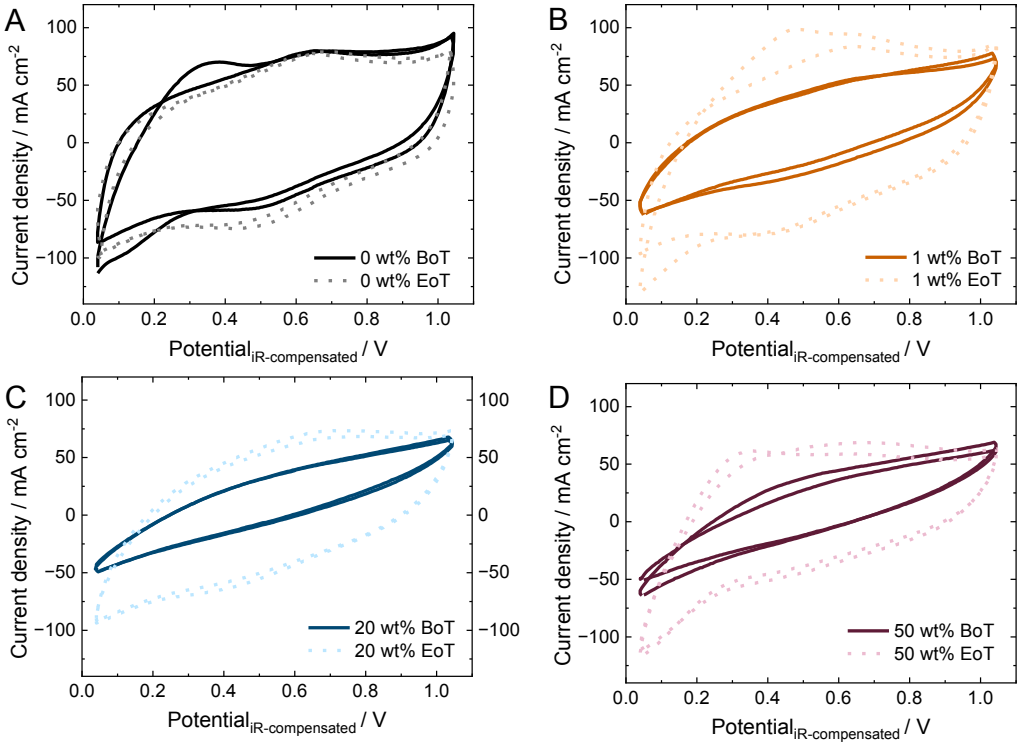

Figure 3. CVs recorded with a scan rate of 100 mA cm^{-2} in GDE half-cell setup at 160 °C with conc. H_3PO_4 electrolyte. CVs of two measurements of GDEs with 0 (A), 1 (B), 20 (C) and 50 wt% (D) Tergitol before (begin of test, BoT) and as dashed lines after (end of test, EoT) recording of the polarization curves are presented.

The uncompensated resistance from impedance spectra at BoT of approx. 0.6 Ω for 0 wt% Tergitol GDE remained similar at EoT. For 1 wt% Tergitol GDE uncompensated resistance of at BoT of 0.9 Ω felt slightly to 0.6 Ω at EoT. The 20 and 50 wt% Tergitol GDEs experience higher resistances in the range of 2.3-2.8 Ω at BoT. At EoT, their resistance felt to approx. 0.6-0.7 Ω, which is similar to 0 and 1 wt% Tergitol GDE. The change in resistance is also reflected in the altered CV curve shapes in Figure 3-B-D. High amounts of non-electronic conductive Tergitol causes higher resistances at BoT. During recording of the polarization curves, Tergitol might be partially leached out from the CL and lead to a decrease in resistance. Additionally, the altered electrolyte coverage at EoT might also decrease the resistance.

Figure 4 depicts the effect of Tergitol on the GDE performance. In Figure 4-A the 0 wt% Tergitol GDE achieves the highest performance. Followed by 1 wt% Tergitol GDE with significant higher overpotentials compared to 0 wt%. The lowest and highly similar performance are revealed by the 20 and 50 wt% GDEs. In Figure 4-B highest activation overpotentials are visible for the 20 wt% Tergitol GDE as the potential at -0.03 mA cm^{-2} reached only 0.57 and 0.63 V. For 50 wt% GDE potentials of 0.66 and 0.81 V_{RHE} are recognized, these fluctuations show instable conditions in terms of electrolyte distribution and catalyst accessibility. At the same current density, potentials of 0.78 and 0.81 V_{RHE} are observed for 1 wt% GDE. Lowest activation overpotential are achieved by 0 wt% GDE, with potential at -0.03 mA cm^{-2} of 0.89 and 0.89 V. This shows that the initial performance of 20 and 50 wt% GDE already suffer in terms of low ORR reaction rate. Since all GDEs

use the same catalyst and comparable catalyst loading, the higher overpotentials of Tergitol treated GDEs is a sign for low catalyst accessibility with low reaction rate.

At higher reaction rates (starting from approx. -15 mA cm^{-2}) ohmic polarization additionally arise and leads to larger overpotentials for 1 wt% than 0 wt% Tergitol GDE, as visible in Figure 4-B. Even higher overpotentials lead to lower performance for the 20 and 50 wt% GDEs. They show the lowest, however similar performance. High amounts of non-electric conductive Tergitol might lead to higher internal resistance of the CL and hence lower performance. EIS analysis already revealed higher resistances with higher Tergitol content as discussed for the CVs. Similar trend is noticed for the polarization curves. TABLE III depicts uncompensated resistance values. With increasing Tergitol content the resistance rises. This indicates higher electric resistance from non-conductive Tergitol within the CL and also emphasizes that Tergitol covers active Fe-N_x sites and decreases the performance.

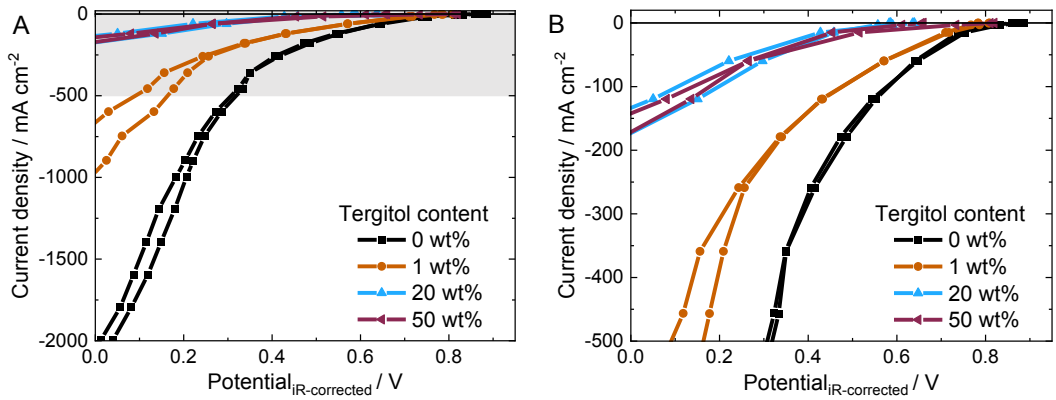

Figure 4. Effect of different Tergitol contents in the CL on the performance GDE half-cell setup at 160 °C with conc. H_3PO_4 electrolyte. A) Full polarization curve is shown and the grey area depicts the area, which is shown enlarged in B).

The reference GDE with 0 wt% Tergitol exhibits the highest power density and reaches a potential of 0.64 ± 0.0 V_{RHE} is at -60 mA cm^{-2} (TABLE III). With 1 wt% Tergitol the potential drops to 0.57 ± 0.0 V_{RHE} at the same current density. The 20 wt% and 50 wt% Tergitol GDEs attain 0.26 ± 0.0 V_{RHE} and 0.26 ± 0.0 V, respectively. The power densities in TABLE III are calculated at -60 mA cm^{-2}. The 1 wt% Tergitol GDE is 11 % lower than the reference without Tergitol. The 20 wt% Tergitol GDE loses 60 % of the power density and 50 wt% GDE loses 59 %, compared to 0 wt% Tergitol GDE. This trend is similar to the contact angle results of the CL with H_3PO_4 at room temperature in Figure 2, where 0 and 1 wt% achieve similar angles and drop by 50 % (20 wt% Tergitol GDE) and 69 % (50 wt% Tergitol GDE) compared to 0 wt% Tergitol GDE. It is clear that with increased surfactant content CL flooding increases and performance decreases.

TABLE III. Average potential of the polarization curve and uncompensated resistance (R) at a current density of -60 mA cm^{-2} and corresponding average power density.

GDE Tergitol content	Potential / V_{RHE}	Ohmic resistance / Ω	Power density / mW cm^{-2}
0 wt%	0.64 ± 0.01	0.54 ± 0.06	38.5 ± 0.0
1 wt%	0.57 ± 0.00	0.82 ± 0.01	34.1 ± 0.0
20 wt%	0.26 ± 0.04	2.3 ± 0.18	15.5 ± 0.2
50 wt%	0.26 ± 0.00	2.0 ± 0.27	15.8 ± 0.0

Conclusion

Our study reveals that the non-ionic surfactants Triton™ X-100 and as alternative the less-hazardous Tergitol™ 15-S-9 similarly affect the Fe-N-C ink sedimentation. For the first time, Fe-N-C-based GDEs with non-ionic surfactant (Tergitol) contents of 0, 1, 20 and 50 wt% in the CL have been characterized towards their wetting characteristic and their performance in the GDE half-cell setup under HT-PEMFC conditions with the following findings:

- Addition of Tergitol does not improve the fabrication of GDE via ultrasonic spray coating.
- The H_2O contact angle decreases with increasing Tergitol content in the Fe-N-C CL. Tergitol increases the CL wettability.
- Without Tergitol the wetting of the CL seems incomplete at room temperature, while Tergitol leads to fully wetted CL already at room temperature.
- A surfactant content starting from 1 wt% lead to electrode flooding by the electrolyte and thus a performance decay in the GDE half-cell measurements. With higher Tergitol content the performance decreases further, due to the increased CL wetting.
- Tergitol covers active Fe-N_x sites and lead to additional performance decay. Furthermore, the electric resistance is increased with increasing Tergitol content in the GDE half-cell measurements.
- A very low content of 1 wt% Tergitol in the CL decreases the GDE performance already.

Other surfactants with ionic or amphoteric properties in low amounts ≤ 1 wt% might positively impact the performance or can shorten activation procedure of Fe-N-C and Pt/Fe-N-C based CLs for HT-PEMFC application. (Partially) removing of the surfactant after GDE fabrication might be beneficial, however, no/less effect of surfactant during operation will be present.

Acknowledgments

This research was carried out in frame of the DLR project LaBreNA funded by Federal Ministry for Economic Affairs and Climate Action and the project HT-PEM 2.0 funded by Federal Ministry for Economic Affairs and Climate Action on the basis of a decision by the German Bundestag, grant number 03ETB016A. We would like to thank Jana Ewert for ICP-MS and SEM measurements. The authors acknowledge the Electron and Light Microscopy Service Unit, Carl von Ossietzky University of Oldenburg for the use of the imaging facilities.

References

1. Q. Meyer, C. Yang, Y. Cheng and C. Zhao, *Electrochem. Energy Rev.*, **6**, 16 (2023).
2. T. Zierdt, J. Müller‐Hülstede, H. Schmies, D. Schonvogel, P. Wagner and K. A. Friedrich, *ChemElectroChem*, **11**, e202300583 (2024).

3. J. Müller-Hülstede, T. Zierdt, H. Schmies, D. Schonvogel, Q. Meyer, C. Zhao, P. Wagner and M. Wark, *J. Power Sources*, **537**, 231529 (2022).
4. N. Seselj, S. M. Alfaro, E. Bompolaki, L. N. Cleemann, T. Torres and K. Azizi, *Adv. Mater.*, **35**, 2302207 (2023).
5. L. Osmieri and Q. Meyer, *Curr. Opin. Electrochem.*, **31**, 2022).
6. Y. Hu, J. O. Jensen, C. Pan, L. N. Cleemann, I. Shypunov and Q. F. Li, *Appl. Catal., B*, **234**, 357 (2018).
7. K. Holst-Olesen, M. Reda, H. A. Hansen, T. Vegge and M. Arenz, *ACS Catal.*, **8**, 7104 (2018).
8. X. P. Wang, M. Ferrandon, J. H. Park, J. J. Shen, A. J. Kropf, H. G. Zhang, P. Zelenay and D. J. Myers, *Electrochim. Acta*, **443**, 2023).
9. N. Pimperl, N. Bevilacqua, M. A. Schmid, P. A. L. Torres, H. A. El-Sayed, R. Zeis and K. P. Zeyer, *J. Power Sources*, **507**, 2021).
10. A. Byeon, K. J. Lee, M. J. Lee, J. S. Lee, I. H. Lee, H. Y. Park, S. Y. Lee, S. J. Yoo, J. H. Jang, H. J. Kim and J. Y. Kim, *ChemElectroChem*, **5**, 1805 (2018).
11. F. Mack, T. Morawietz, R. Hiesgen, D. Kramer, V. Gogel and R. Zeis, *Int. J. Hydrogen Energy*, **41**, 7475 (2016).
12. W. J. Lee, J. S. Lee, H. Y. Park, H. S. Park, S. Y. Lee, K. H. Song and H. J. Kim, *Int. J. Hydrogen Energy*, **45**, 32825 (2020).
13. F. Mack, M. Klages, J. Scholta, L. Jorissen, T. Morawietz, R. Hiesgen, D. Kramer and R. Zeis, *J. Power Sources*, **255**, 431 (2014).
14. J. Halter, T. Gloor, B. Amoroso, T. J. Schmidt and F. N. Buchi, *Physical Chemistry Chemical Physics*, **21**, 13126 (2019).